

## Fast and Controlled Integration of Carbon Nanotubes into Microstructures

Wenjun Xu<sup>1</sup>, Chang-Hyeon Ji<sup>2</sup>, Richard Shafer<sup>2</sup>, Mark G. Allen<sup>2</sup>

<sup>1</sup>Department of Polymer, Textile and Fiber Engineering,

<sup>2</sup>Department of Electrical Engineering, Georgia Institute of Technology, 791 Atlantic Drive, Atlanta, GA, 30032, U.S.A.

### ABSTRACT

In this paper, we report the results of a rapid and room temperature integration approach for the selective and structured deposition of carbon nanotubes (CNTs) into three-dimensional microstructures. The approach exploits electrophoretic deposition (EPD) from an aqueous suspension of CNTs, together with suitably patterned and electrically-energized microstructure-bearing substrates. Uniform 2-D and 3-D micropatterns of CNTs on wafer scale have been achieved in less than 4 minutes with controllable thicknesses ranging from 133nm to several micrometers. Orientation of the deposited CNTs was observed in microstructures with certain dimensions. Surface hydrophobicity of the microstructures was found to be critical in achieving well-defined micropatterning of CNTs. A hydrophobic microstructure surface leads to the selective patterning profiles of CNTs, while a hydrophilic surface induces CNTs assembly over the entire microstructure, with resultant loss of selectivity. This approach can be further extended to fabricate 3-D micropatterns with multilayer materials on flexible substrate through the aid of transfer micromolding techniques.

### INTRODUCTION

CNTs have been intensively investigated since 1991 and exhibit promising potential in fields such as molecular electronics, microsensors, solar cells, field emission devices and biocoatings [1-5]. This high aspect ratio nanomaterial possesses interesting piezoresistive, electrical, physiochemical and mechanical properties that can serve as a key enabler in microsystems such as microsensors and microactuators [6-8]. To integrate this versatile material into miniature systems, suitable approaches are required for localizing CNTs in certain desired areas of the microstructure. In general, there are two approaches to achieve this localization: during CNT synthesis, and post-CNT synthesis. The former approach usually involves pre-patterning of catalyst at the desired sites, followed by a high temperature growth reaction. Although this approach deposits the nanotubes in a desired area directly, the high temperature required as well as the inability to refine the CNTs prior to deposition are potential limitations. The latter approach overcomes both of these limitations, at the expense of extra processing steps.

There has been much previous work to pattern CNTs on substrates using a post-synthetic approach. Terranova et. al. reported assembly of CNTs across micron-sized gaps between electrodes via dielectrophoresis under AC field [9]. Cui utilized polymer-assisted self-assembly to obtain CNT layers on microstructures [10]. An AFM tip has also been used to place individual CNTs onto desired locations in nanodevices.

Good control of the thickness and morphology of CNTs is also important for quantitatively studying their properties in micro-systems and optimize the performance of resultant devices. Electrophoretic deposition (EPD), a technique in which electric fields are used to assist the transport of charged species, has been demonstrated to be capable of uniformly depositing CNTs with controlled mass into large substrates at room temperature, and is a facile, fast and cost effective process [11].

In the present study, the use of EPD approaches together with substrates bearing suitably patterned microstructures was adopted to investigate the selective deposition of CNTs onto large areas in a single step. Three different microstructures were investigated and their suitability for selective CNT deposition evaluated. Uniform 2-D and 3-D micropatterns were successfully generated in less than 4min at room temperature. The assembly behavior and morphology of the CNTs were studied and the effect of surface hydrophobicity of the microstructures was found to be a critical factor for achieving selective deposition.

## THEORY AND EXPERIMENT

MWCNTs (Nanostructured & Amorphous Materials, Inc. 95+%) were acidified in a mixture of sulfuric acid and nitric acid (3:1 volume ratio) for 4h through sonication at room temperature. Carboxyl acid groups were thereby introduced into the nanotubes; these acid groups were utilized both to facilitate the EPD, as well as to improve the dispersion of the CNTs in aqueous solution. Three geometric types of microstructures were fabricated on silicon substrates. The first microstructure consisted of interdigitated gold microelectrode arrays, in which the electrodes were deposited on a dielectric layer which was formed on top of the silicon. The second microstructure consisted of microchannels, formed in photoresist, atop a conducting gold layer that had been deposited atop a silicon-nitride-bearing silicon wafer. The third microstructure was similar to the microchannel structure, but instead was fabricated from SU-8 epoxy and consisted of circular wells instead of channels. MWCNTs-COOH were then dispersed in water at a concentration of 0.1mg/ml. The microstructure-bearing substrates and a copper counterelectrode were immersed in the CNT dispersion and electrically energized with an external voltage source, with the copper serving as cathode and substrate serving as anode. The negatively-charged CNTs-COO<sup>-</sup> were then electrically directed in water into the microstructures under a constant electric field of 20V/cm applied across two electrodes for various times.

The deposited mass,  $M$ , can be estimated by the equation 1 [12]:

$$M = \int_0^t \alpha A \mu E c dt \quad (1)$$

where  $\alpha$  is the mass fraction of material deposited on the electrode,  $A$  is the area of the electrode,  $\mu$  is the material mobility,  $E$  is the applied electric field, and  $c$  is the material concentration in the dispersion. To achieve localized deposition of CNTs on the microscale, it is observed that low  $c$  and  $E$  are preferred. These two parameters also determine the thickness of the CNTs layer since  $A$ ,  $\mu$  and  $c$  are constants for a given microstructure/dispersion combination.

The morphology of the CNT patterns was characterized by Zeiss Scanning Electron Microscopy (SEM) Ultra60. Atomic force microscopy (AFM, MultiMode and Dimension 3000, Veeco Metrology) was used for topography and surface roughness study of the SU-8

microstructures before and after oxygen plasma treatment. Static contact angle measurements were performed with a sessile drop method for the surface hydrophobicity test. WVASE32 Woollam Ellipsometer was utilized to study the thickness of the CNTs layer on the microelectrodes.

## DISCUSSION

### Assembled micropatterns of CNTs in microstructures

The micropatterns generated by EPD as deposited in various microstructures are shown in Figure 1. When no substantial topography was present in the microstructures, the resultant CNT micropatterns typically assembled only onto those conductive metal areas to which electric fields had been applied. The negatively charged CNTs were neutralized and aggregated when reaching those surfaces. It was also observed that immediately adjacent conductive metal areas that were not energized exhibited no deposition. Figure 1a and 1d confirm that CNTs did not assemble on

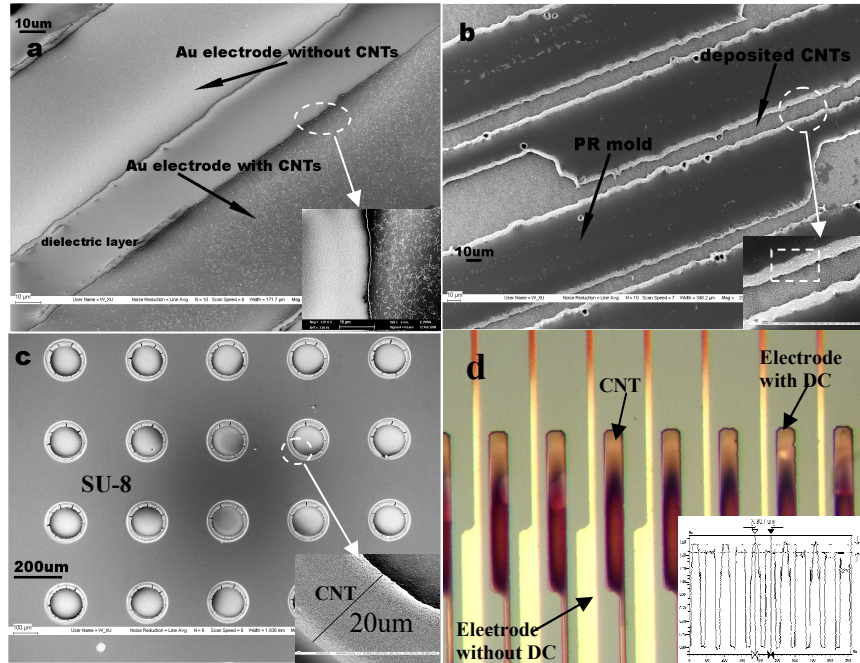


**Figure 1.** SEM images of CNTs assembly in (a) interdigital microelectrodes, (b) photoresist (PR) microchannels, (c) SU-8 microwell arrays and (d) optical image of the CNTs patterns in microelectrodes, the insert shows an electrode thickness measurement, illustrating the height difference between deposited and non-deposited electrodes.

any micropatterns lacking an applied electric field. Similarly, no deposition was observed on the dielectric materials adjacent to and between the metal areas. The thickness of the deposited CNT layer was approximately 133nm as illustrated in Figure 1d (insert), corresponding to approximately two to three layers of CNTs since the diameter of the CNTs is 50~80 nm. As observed in Figure 1c, CNTs assembled conformally around the microwell inner surface and in addition generated a 20um wide circular belt framing the well opening, thereby creating a continuous 3-D coating in each isolated microwell. Similar assembly behavior was observed in the rectangular microchannels as shown in Figure 1b, where conformal assembly on the channel

inner surface and a 5-10 $\mu\text{m}$  wide rectangular CNTs belt framing the channel was generated. These observations indicate that under these conditions, the deposition of CNTs is in accordance with the conformal coating nature of the EPD process.

### **Alignment of CNTs**

CNTs have been reported to align perpendicular to the electrode substrate (i.e., parallel to the external field lines) under high electric [13] and magnetic fields [14]. In the present study, the CNTs were found to undergo oriented assembly in the rectangular channel and microwell structures when these microstructures were of sufficiently small dimensions (15 $\mu\text{m}$  and 3 $\mu\text{m}$ , respectively). For the microchannel structures, the CNTs formed a dense and one dimensional assembly transversely at the bottom of the channel, and also tended to assemble in a parallel fashion on the sidewall of the channel, as observed in Figure 2a. For the microwell structures, the CNTs tend to form a coating around the circular opening in a way that is parallel with the sidewall without clogging the opening, as well as circumferentially within the well, as shown in Figure 2b. However, this orientation effect was only observed in microstructures having openings with relatively small dimensions. For microstructures with larger dimensions, the CNTs seem to assemble in a much less oriented or random manner.

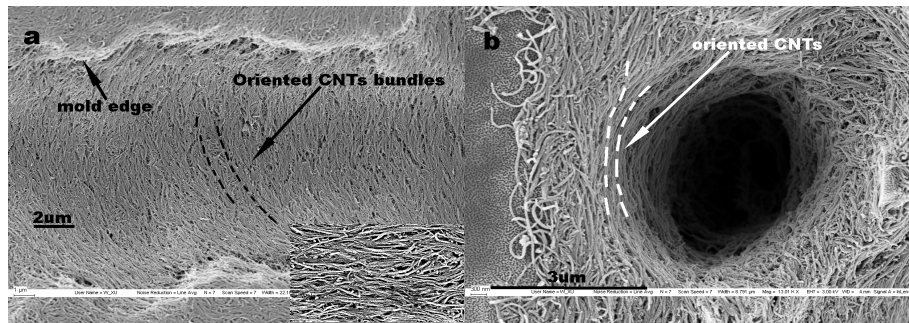


**Figure 2.** SEM images of aligned CNTs in (a) micro-channel and (b) circular well opening.

### **Effect of surface hydrophobicity on selectivity of CNT assembly**

The surface hydrophobicity of the non-conducting layers, including the top surface exposed to the dispersion, was found to play a significant role in the selective integration of CNTs into microstructures. In the case of interdigitated microelectrodes, the dielectric layer, which is underneath and between the microelectrodes (Figure 1a), was exposed to a brief (i.e., insufficient to completely remove the dielectric layer) hydrofluoric acid (HF) aqueous solution during the electrode patterning process. The contact angle of the dielectric layer after the process decreased significantly as shown in Table I. This rise of the hydrophilicity results in the continuous deposition of the CNTs over the whole microstructure, including the non-conductive dielectric region.

**Table I.** Contact angle of the dielectric layer

	contact angle without HF etching	contact angle after HF etching
parylene	86.47°	59.54°
SiC	86.05°	43.88°
SiN <sub>x</sub>	63.92°	40.41°
SiO <sub>2</sub>	38.78°	<10°

This may be due to the fact that CNTs aqueous solution can form a good interface with the hydrophilic surface where the moving CNTs under dc field collide and aggregate with those in the interface layer. This negative effect can be reduced by changing the microelectrode patterning process from etching to lift-off. In this case, the hydrophobicity of the dielectric layers was preserved and 2-D pattern of CNTs on microelectrodes can be achieved as shown in Figure 1a with parylene as the dielectric layer.

A similar hydrophobicity effect was revealed in patterning CNTs into SU-8 microwell arrays. The surface topography of the pristine SU-8 before and after plasma treatment is shown in AFM images in Figure 3. Oxygen plasma increases the surface roughness of the SU-8 from 0.289nm

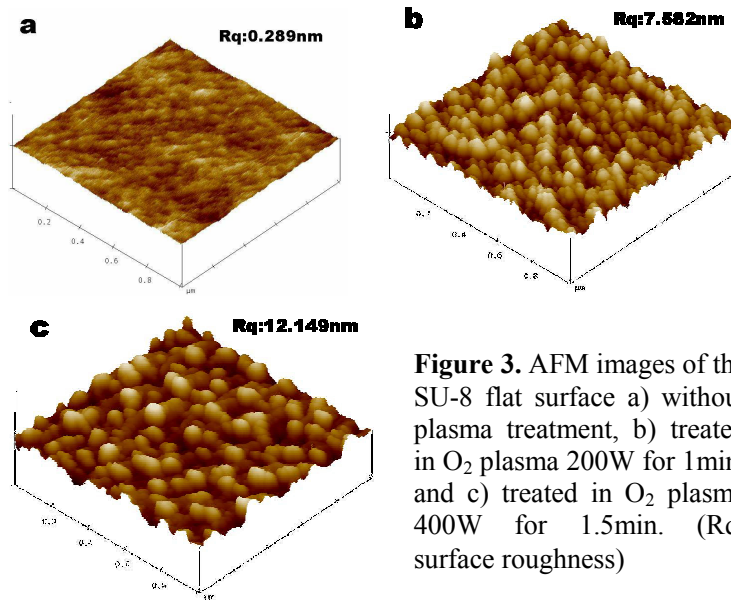


**Figure 3.** AFM images of the SU-8 flat surface a) without plasma treatment, b) treated in O<sub>2</sub> plasma 200W for 1min, and c) treated in O<sub>2</sub> plasma 400W for 1.5min. (Rq: surface roughness)

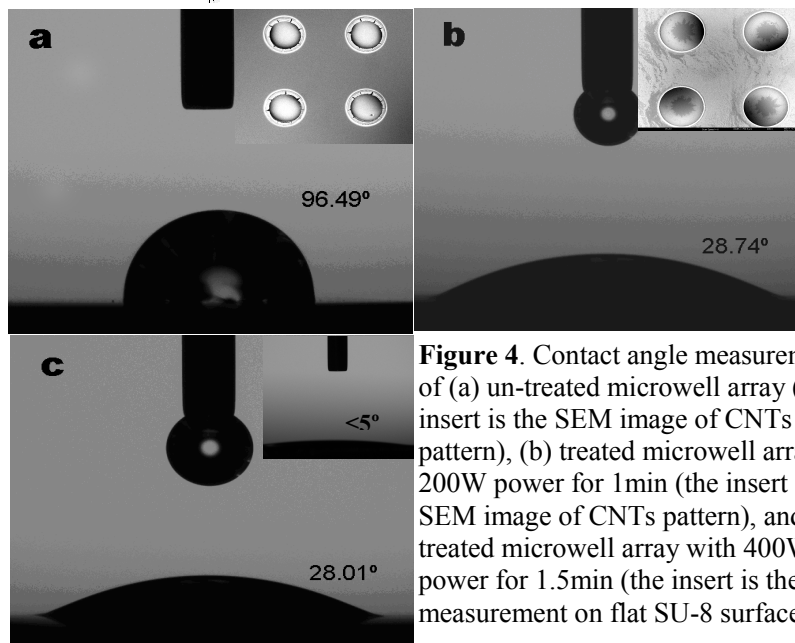


**Figure 4.** Contact angle measurements of (a) un-treated microwell array (the insert is the SEM image of CNTs pattern), (b) treated microwell array with 200W power for 1min (the insert is the SEM image of CNTs pattern), and (c) treated microwell array with 400W power for 1.5min (the insert is the measurement on flat SU-8 surface).

up to 12.149nm. The contact angle of the micropattern dropped from 96.49 ° to 28 °, that is, the surface turned from hydrophobic to hydrophilic. The CNTs then formed a coating over the whole SU-8 microstructure (SEM image insert in Figure 4b) instead of generating a well-defined micropattern in each isolated microwell (SEM image insert in Figure 4a). Another observation is that the microwell patterns exhibit higher hydrophobicity than the flat SU-8 surface in all three stages. As illustrated in Figure 4c, after the oxygen plasma treatment, the contact angle is 28 ° for the microstructure region and is close to 0 ° for a flat (i.e., non-microstructured region) in the field of the wafer. This is believed to be similar to a structure-induced hydrophobicity.

## CONCLUSIONS

Uniform 2-D and 3-D micropatterns of CNTs over wafer-scale areas have been successfully achieved via EPD from water-based dispersions. The deposition time was typically less than 4 minutes at room temperature, with controllable CNT layer thicknesses ranging from 133nm to the micrometer range. Under appropriate deposition conditions, CNTs assembled conformally around the microwell inner surface and generated a 20um wide circular belt around the well opening, creating a continuous 3-D coating in each isolated well. Similar assembly behavior was revealed in rectangular microchannels, where a rectangular CNT belt was generated around the channel opening. The surface hydrophobicity of the non-conductive regions in microstructures is critical for the selective micropatterning of CNTs.

## REFERENCES

1. K. Jensen, K. Kim, and A. Zettl, *Nature Nanotechnology* **3**, 533(2008).
2. T. Kawano, H. C. Chiamori, M. Suter, Q. Zhou, B.D. Sosnowchik, and L. Lin, *Nano Lett.* **7**, 3686 (2007).
3. S. Berson, R. de Bettignies, S. Bailly, S. Guillerez, and B. Joussetme, *Adv. Funct. Mater.* **17**, 3363(2007).
4. P. Rai, D. R. Mohapatra, K. S. Hazra, D. S. Misra, and S. P. Tiwari, *Appl. Phys. Lett.* **93**, 1921 (2008).
5. A. R. Boccaccini and Q. Chen, *Adv. Funct. Mater.* **17**, 2815 (2007).
6. R. J. Grow, Q. Wang, J. Cao, D. Wang, and H. Dai, *Appl. Phys. Lett.* **86**, 093104 (2005).
7. N. Chang, C. Su, and S. Chang, *Appl. Phys. Lett.* **92**, 063501 (2008).
8. J. Tong and Y. Sun, *Nanotechnology*, **6**, 519(2007).
9. M.L Terranova and A.D. Carlo, *J. Phys: Condens. Matter.* **19**, 225004 (2007).
10. W. Xue and T. Cui, *Sensors and Actuators A: Physical* **136**, 510 (2007).
11. R. B. Aldo and S.P.S. Milo, *Carbon* **44**, 3149 (2006).
12. M. Guduru, A. Francis, T. A. Dobbins, *Mater. Res. Soc. Symp. Proc.* **858E**, HH13.29.1 (2005).
13. C. Ma, W. Zhang, Y. Zhua, Li. Jia, R. Zhanga, N. Koratkarb, J. Liang, *Carbon* **46**, 706 (2008).
14. K. Kordas, T. Mustonen, G. Toth, J. Vahakangas, A. Uusimaki, H. Jantunen, A. Gupta, K. V. Rao, R. Vajtai, and P. M. Ajayan, *Chem. Mater.* **19**, 787(2007).